Journal of Heat and Mass Transfer Research

Semnan University

Numerical Study of Flow and Heat Transfer Characteristics of CuO/H₂O Nanofluid within a Mini Tube

Mohammad Reza Aminian[a], Ali Reza Miroliaei[a]*, Behrooz Mirzaei Ziapour[b]

a Department of Chemical Engineering, University of Mohaghegh Ardabili, Ardabil, Iran.
b Department of Mechanical Engineering, University of Mohaghegh Ardabili, Ardabil, Iran.

ABSTRACT

Nanofluids are new heat transfer fluids, which improve thermal performance while reducing the size of systems. In this study, the numerical domain as a three-dimensional copper mini tube was simulated to study the characteristics of flow and heat transfer of CuO/H₂O nanofluid, flowed horizontally within it. The selected model for this study was a two-phase mixture model. The results indicated that nanofluids with the platelet nanoparticles have better thermal performance than other shapes of nanoparticles such as cylindrical, Blade, Brick, and spherical nanoparticles, respectively. By studying the flow characteristics, it was found that the pressure drop and friction factor of the nanofluids are dependent on the shape of the nanoparticles so that the nanofluids containing spherical nanoparticles have the lowest reduction in the friction factor and nanofluids containing platelet-shaped nanoparticles have the highest reduction in friction factor. Furthermore, as new formulas, two correlations were suggested to calculate the Nusselt number of nanofluids according to the effect of nanoparticle shape on the laminar and turbulent flow regimes.

1. Introduction

Nanofluids are a new class of heat transfer fluids provided by adding solid particles (in nanoscale) to a base fluid [1]. They are utilized in many types of equipment such as transportation, micro-electronics, defense weaponry, nuclear reactors, heat exchangers, utilization of solar energy for power generation, and so on [2, 3]. Both thermal conductivity and viscosity of nanofluids would increase by adding nanoparticles, which cause the enhancement of energy demand for pumping power in the systems [4, 5]. Therefore, other effective parameters in the enhancement of the heat transfer coefficient and decreasing viscosity of the nanofluids must be studied. One of the effective parameters is the nanoparticle shape [6]. In most studies, the spherical nanoparticles have been used in the base fluid, whereas at least 70% of the raw materials consist of non-spherical particles in modern industries [7]. Consequently, this explains the importance of studying the nanoparticle shape effect. Several studies have been conducted on the effect of nanoparticle shape,

both numerically and experimentally. For instance, Xie et al. [8] reported that the thermal conductivity of nanofluids with the cylindrical nanoparticles is better than that of the spherical nanoparticles. Murshed et al. [9] conducted a study using TiO₂ rod-shaped nanoparticles. Their results showed that the size and the shape of nanoparticles increase the thermal conductivity of the nanofluid. Timofeeva et al. [10] investigated the shape effect of alumina nanoparticles on the thermal conductivity and viscosity of nanofluids. They found that the effective thermal conductivity of the nanofluids is proportional to the total surface area of nanoparticles. Elias et al. [11] studied the nanoparticle shape effect on the heat transfer coefficient in a shell and tube heat exchanger. Their results indicated that cylindrical nanoparticles have better heat transfer coefficient than the other shapes. The effect of SiO₂ nanoparticle shape on the heat transfer and fluid flow characteristics was evaluated by Vanaki et al. [12]. It was known that the Nusselt number of nanofluid, including platelet nanoparticles, is the highest. The effects of

* *Corresponding Author: A. R. Miroliaei, Department of Chemical Engineering, University of Mohaghegh Ardabili, Ardabil, Iran.*
Email: armiroliaei@uma.ac.ir

Reynolds number, particle volume fraction, and aspect ratio of the nanoparticles on the heat transfer coefficient and friction factor of nanofluids with rod-like nanoparticles were investigated by Lin et al. [13]. They reported that the velocity gradient varies in two ends of nanoparticle that caused the heat transfer increases. Furthermore, they explained that the nanofluid viscosity increases with increasing the particle aspect ratio; consequently, heat transfer coefficient and Nusselt number decrease. The thermal performance of a non-Newtonian nanofluid was studied by Bahiraei et al. [14]. They stated that the pressure drop and heat transfer coefficient of the nanofluid would increase with increasing the concentration and reducing the particle size. Naphon and Wiriyasart [15] investigated the effect of pulsating flow and magnetic field on the heat transfer in a micro-fine tube. Their results indicated that the pulsing flow and magnetic field would affect the Brownian motion of nanoparticles. The effect of geometry type on the flow charactristics and thermal performance of hybrid nanofluids was studied by Bahiraei and Mazaheri [16]. They found that pressure drop and heat transfer coefficient of hybrid nanofluids in the chaotic twisted channel are more than those of simple channel.

The present study states the effect of nanoparticle shapes such as spherical, cylindrical, brick, blade and platelet on the heat transfer and flows characteristics of CuO-water nanofluids in a mini tube using a two-phase mixture model. Finally, based on the simulation results, two correlations based on the effect of nanoparticle shape will be suggested to calculate the Nusselt number.

2. Numerical simulation

2.1. Model geometry

Figure 1 shows the computational domain as a three-dimensional straight tube with 970 mm length and 4.5 mm inner diameter according to the experiment setup in the work of Wen and Ding [17].

2.2. Governing equations

2.2.1. Mixture model

The single-phase and two-phase models have been utilized by many researchers [11, 12, 18]. According to the literature, the results of two-phase models are better than those of a single phase model [19, 20]. In the mixture model, it is assumed that the velocity of each phase is independent of another phase. In this theory, the equations are solved for the mixture and are also utilized for each phase. Therefore, the total equations used to determine the fluid flow and temperature characteristics are as follows [6, 21]:

Continuity equation:
$$\nabla.\left(\rho_m \vec{V}_m\right) = 0 \qquad (1)$$
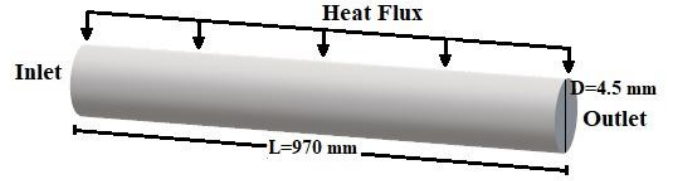

Figure 1. Schematic of the computational domain

where, ρ_m and $\vec{V}_m$ are mixture density and mass averaged velocity, respectively.

Momentum equation:

$$\nabla.\left(\rho_m \vec{V}_m \vec{V}_m\right) = -\nabla P_m + \mu_m \nabla^2 \vec{V} \qquad (2)$$
$$-\nabla.\left(\sum_{k=1}^{n} \varphi_k \rho_k \overline{v_k v_k}\right)$$
$$+\nabla.\left(\sum_{k=1}^{n} \varphi_k \rho_k \vec{V}_{dr,k} \vec{V}_{dr,k}\right)$$
$$-\rho_m \beta_m (T - T_0) g$$

In the above equilibrium, $\vec{V}_{dr,k}$ is the drift velocity of the kth phase. The drift velocity for the second phase is obtained from Eq. (3):

$$\vec{V}_{dr,p} = \vec{V}_{pf} - \sum_{k=1}^{n} \frac{\varphi_k \rho_k}{\rho_m} \vec{V}_{fk} \qquad (3)$$

Manninen et al. [19] proposed Eq. (4) for determining the relative velocity:

$$\vec{V}_{pf} = \frac{\rho_p d_p^2}{18 \mu_f f_{drag}} \frac{(\rho_p - \rho_m)}{\rho_p} a \qquad (4)$$

Also, the drag function f_{drag} is calculated from Schiller and Naumann equations [23]:

$$f_{drag} = \begin{cases} 1 + 0.15 Re_p^{0.687} & Re_p \leq 1000 \\ 0.0183 Re_p & Re_p > 1000 \end{cases} \qquad (5)$$

a, in Eq. (4) is defined as follows:
$$a = g - (\vec{V}_m.\nabla)\vec{V}_m \qquad (6)$$

Energy equation:

$$\nabla.\left(\sum_{k=1}^{n} \varphi_k \vec{V}_k (\rho_k H_k + P)\right) = \nabla.\left(k.\nabla T - C_p \rho_m \overline{v}t\right) \qquad (7)$$

in which k is the thermal conductivity coefficient.

In addition to the above equations, the volume fraction equation is also solved for the second phase:

$$\nabla.\left(\varphi_p \rho_p V_m\right) = -\nabla.(\varphi_p \rho_p V_{dr,p}) \qquad (8)$$

Finally, with solving all equations, the local mean heat transfer coefficient and the local mean Nusselt number are determined as follow:

$$h = \frac{q_w''}{T_w - T_m} \qquad (9)$$

$$Nu = \frac{hD}{k_{nf}} \qquad (10)$$

In the above equations, the wall and fluid averaged temperatures are used to calculate T_w and T_m, respectively.

2.3. Boundary conditions and numerical method

The uniform axial velocity profile based on the Reynolds number and the constant temperature of 295 K was used in the tube inlet. No slip boundary condition and constant heat flux were applied to the tube wall. For the tube outlet, it was assumed that the flow and temperature fields are developed, i.e. all axial derivatives are zero. In the turbulent flow regime, the model of the k-ε standard with the enhanced wall treatment was used.

The numerical method based on the finite volume method was applied to solve the governing equations. The velocity and pressure were coupled with the SIMPLE algorithm. The second-order upwind method was also used for discretization of convective terms in all equations. It was assumed that the residuals are smaller than 10-7.

2.4. Thermophysical properties

The thermophysical properties of CuO and $\gamma-Al_2O_3$ nanoparticles and base fluid (H_2O) are presented in Table 1.

The following equations have been proposed to calculate the thermophysical properties of nanofluids:

Density [17]:

$$\rho_{nf} = (1-\varphi)\rho_{bf} + \varphi\rho_p \qquad (11)$$

ρ_{bf} and φ are the base fluid density and nanoparticle volume fraction, respectively.

Heat capacity [25]:

$$C_{p,nf} = \frac{(1-\varphi)\rho_{bf}C_{p,bf} + \varphi\rho_p C_{p,p}}{\rho_{nf}} \qquad (12)$$

Thermal conductivity:

The effective thermal conductivity would be calculated using Hamilton-Crosser model [10]:

$$k_{nf} \qquad (13)$$
$$= \frac{k_p + (n-1)k_f - (n-1)\varphi(k_f - k_p)}{k_p + (n-1)k_f + \varphi(k_f - k_p)}k_f$$

where n is the empirical shape factor given by Eq. (14):

$$n = \frac{3}{\psi} \qquad (14)$$

in which, ψ is the sphericity defined as the ratio between the surface area of the volume equivalent sphere and the surface area of the particle.

Dynamic viscosity [10]:

Table 1. Thermophysical properties of nanoparticle and base fluid [24].

Thermophysical properties	water	Al2O3	CuO
$\rho(\frac{kg}{m^3})$	998.2	3970	6320
$C_p(\frac{J}{kg.k})$	4182	765	531.8
$k(\frac{w}{m.k})$	0.6	40	76.5
$\mu(\frac{N.s}{m^2})$	0.001003	-	-

Table 2. The value of parameters in Eqs. (14) and (16) [10].

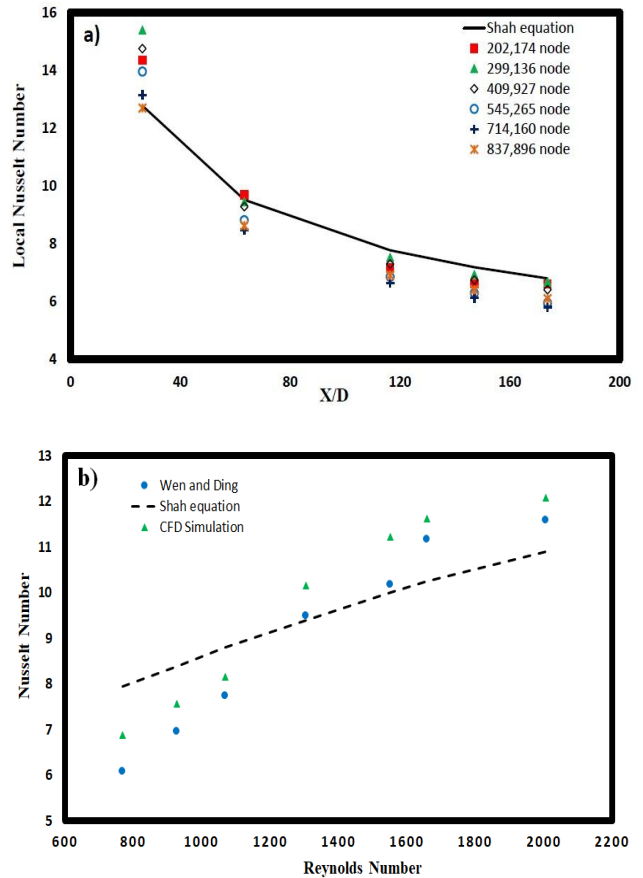| Type of nanoparticle	Sphericity (ψ)	A_1	A_2
Cylinders	0.62	13.5	904.4
Bricks	0.81	1.9	471.4
Blades	0.36	14.6	123.3
Platelets	0.52	37.1	612.6

Figure 2. Comparison of CFD results with experimental data and empirical correlations in laminar flow regime
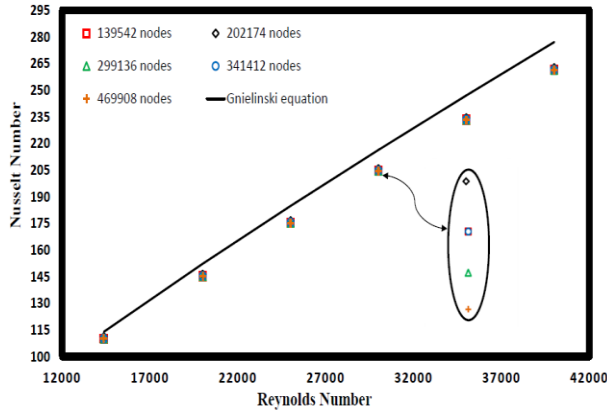
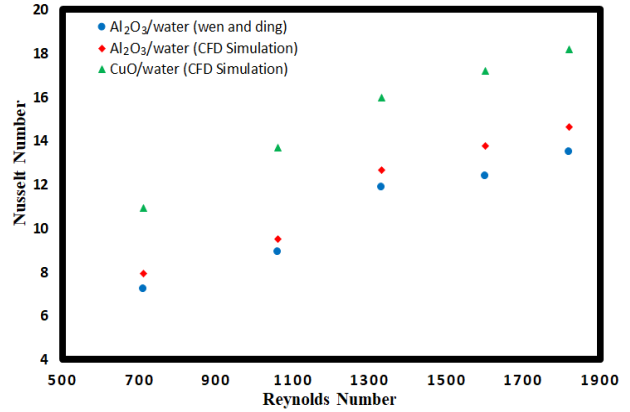**Figure 3.** Comparison of CFD results with empirical correlations in turbulent flow regime

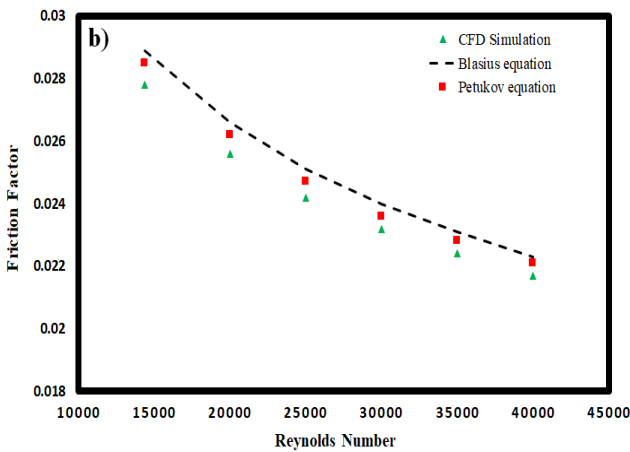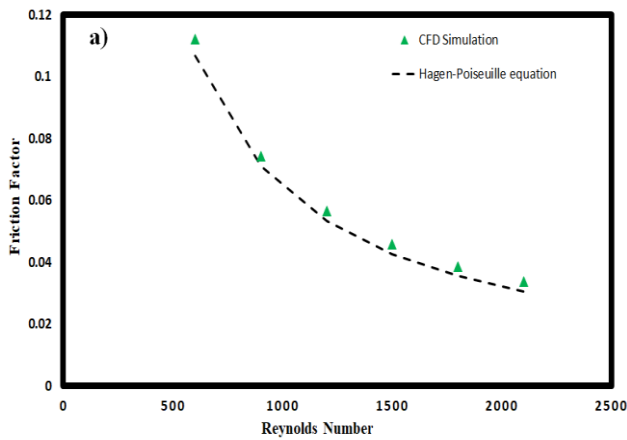**Figure 5.** Comparison of CFD simulations with experimental data for two nanoparticles of CuO and $\gamma-Al_2O_3$ at x/D = 63.

Figure 4. Comparison of CFD friction factor with empirical correlations: a) Laminar flow b) Turbulent flow.
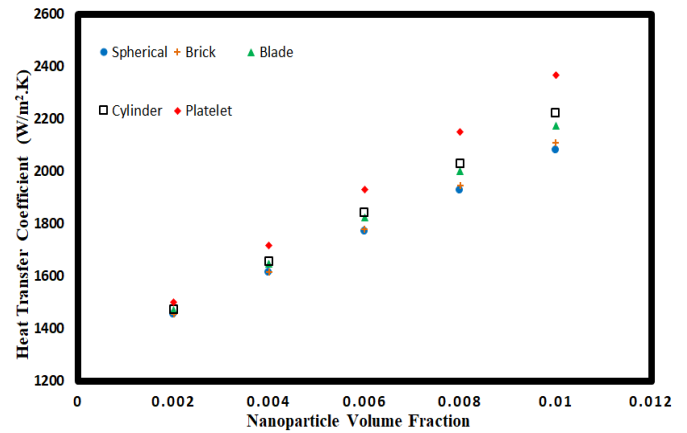

Figure 6. Heat transfer coefficient versus nanoparticle volume fraction with different nanoparticle shapes at Re = 1200.

The particle sphericity and the value of A_1 and A_2 coefficients are mentioned in Table 2.

3. Results and discussion

3.1. Model validation

A grid independence study was performed for the 3D mini-tube using water-based fluid. In the laminar flow regime, six grids were selected. The number of nodes in these grids is 202174, 299136, 409927, 545265, 714160 and 837896 nodes. The CFD results were compared with experimental data of Wen and Ding [19] and predictions of Shah's equations [26] and Eq. (18) [5]:

$$Nu \qquad (17)$$

$$= \begin{cases} 1.953(RePr\frac{d}{x})^{1.3} & (RePr\frac{d}{x}) \geq 33.3 \\ 4.364 + 0.0722RePr\frac{d}{x} & (RePr\frac{d}{x}) < 33.3 \end{cases}$$

$$\mu_{nf} = (1 + 2.5\varphi)\mu_{bf} \qquad \text{(spherical nanoparticle)} \qquad (15)$$

$$\mu_{nf} = \mu_{bf}(1 + A_1\varphi + A_2\varphi^2) \qquad \text{(non-spherical anoparticle)} \qquad (16)$$
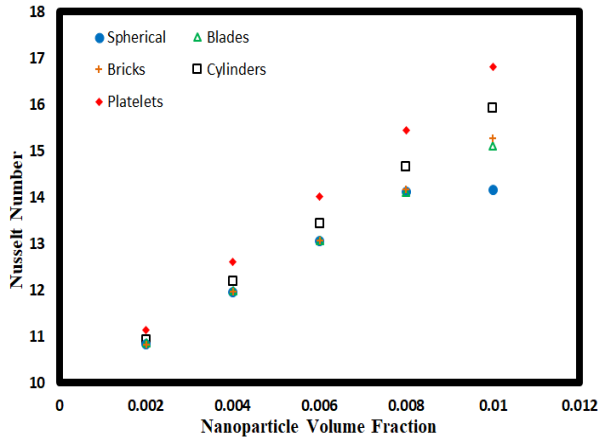
Figure 7. Nusselt number versus nanoparticle volume fraction with different nanoparticle shapes at Re = 1200.
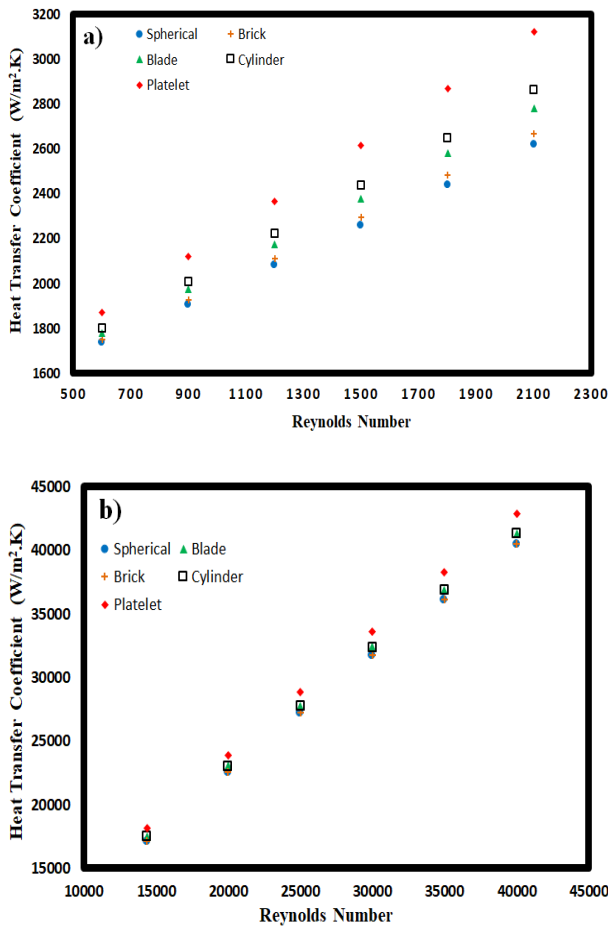

Figure 8. Heat transfer coefficient versus Reynolds number with different nanoparticle shapes in 1 % nanoparticle volume fraction: a) Laminar flow b) Turbulent flow

$$Nu \qquad\qquad (18)$$
$$= 0.4328(1.0$$
$$+ 11.285\varphi^{0.754}Pr_d^{0.218})Re^{0.333}Pr^{0.4}$$

According to Figs. 2(a) and 2(b), it is known that the grid size of 299136 nodes is suitable to get satisfactory results.

In the turbulent flow regime, five grids with the number of 139542, 202174, 299136, 341412, and 469908 nodes were selected. The reliability and accuracy of the numerical results were carried out using the Gnielinski equation [27]:

$$Nu = 0.012(Re^{0.87} - 280)Pr^{0.4} \qquad\qquad (19)$$

As it can be seen in Fig. 3, the number of 202174 nodes would give the closest result to Gnielinski's equation.

Furthermore, the friction factor results were compared to Hagen–Poiseuille's equation in the laminar flow regime and equations of Blasius [28] and Petukov [29] in the turbulent flow regime:

$$f = \frac{64}{Re} \qquad \text{(Hagen–Poiseuille equation)} \qquad (20)$$

$$f = \frac{0.316}{Re^{0.25}} \qquad \text{(Blasius equation)} \qquad (21)$$

$$f = (0.790\ln(\text{Re}) - 1.64)^{-2} \qquad \text{(Petukov quation)} \qquad (22)$$

According to Figs. 4(a) and 4(b), it is observed that the numerical results of friction factor have good agreement with those of the proposed correlations. As can be seen from these figures, the average error between CFD and the above equations is less than 10%.

Fig. 5 shows the comparison of CFD simulations with the experimental data of Wen and Ding [17] for two types of nanoparticles of CuO and γ −Al$_2$O$_3$. It is found that the Nusselt number of CuO nanoparticle is more than that γ −Al$_2$O$_3$ nanoparticle.

3.2. Nanoparticle shape effect

In the next sections, the nanoparticle shape effect on the heat transfer coefficient and flow characteristics with changing nanoparticle concentration and Reynolds number is evaluated in two flow regimes. The CFD simulations are expressed for five nanoparticle shapes such as spherical, cylindrical, brick, blade, and platelet. Fig. 6 shows the variation of the heat transfer coefficient with increasing the volume fraction of CuO nanoparticle in the water base fluid. As can be seen, with increasing the volume fraction of the nanoparticle, the thermal conductivity of nanofluid increases, which causes an increase in the heat transfer coefficient of nanofluid. The increasing nanoparticle volume fraction also causes that the temperature of the tube wall decreases, and consequently, the temperature gradient between the nanofluid and the tube wall increases. However, excessive addition of nanoparticles to the base fluid leads to an increase in the nanofluid viscosity and increases the thickness of the thermal boundary layer that is one of the important factors in reducing the transferred heat. In this case, there is the probability of sedimentation and damage to the equipment indicating the importance of the shape effect of the nanoparticles on the heat transfer coefficient. According to Fig. 6, as mentioned before, it could be observed that the heat transfer coefficient increases with increasing the volume fraction of

nanoparticle, and platelet nanoparticle have the most heat transfer coefficient compared to other nanoparticles.

The nanoparticle volume fraction effect on the Nusselt number of nanofluids with different shapes of nanoparticle has been shown in Fig. 7. It is found that the Nusselt number of nanofluids increases with increasing the volume fraction. Hence, the platelet nanoparticle has the most Nusselt number compared with cylindrical, blade, brick, and spherical nanoparticles, respectively. It is known that in the volume fraction less than 0.004, the thermal performance of nanofluid with spherical nanoparticle is better than that with the brick nanoparticle. Moreover, it is seen that with increasing the volume fraction from 0.008 to 0.01 in the nanofluid containing spherical nanoparticles, the Nusselt number increases about 0.32% while in the nanofluid containing the platelet nanoparticles in the volume fraction of 0.008, the Nusselt number increases about 9.41%. This means that the heat transfers could be increased by changing the shape of the nanoparticles without increasing the volume fraction of nanoparticles.

The Reynolds number effect on the heat transfer coefficient is shown in Figs. 8(a) and 8(b) in laminar and turbulent flow regimes. As shown in these figures, the heat transfer coefficient of the nanofluids increases with increasing the Reynolds number. It is also observed that the platelet nanoparticle has the best thermal performance compared to other nanoparticles. The numerical results of the Nusselt number are also compared with Eqs. (17) and (18) in the laminar flow regime and Eq. (19) in turbulent flow regime. Figs. 9(a) and 9(b) indicate that the Nusselt number increases with increasing the Reynolds number. It is seen that the platelet nanoparticle has the most Nusselt number and subsequently, the nanoparticles of cylindrical, blade, brick, and spherical, respectively.

It is found from Figs. 9(a) and 9(b) that the CFD results of spherical nanoparticle are very close to those of the common equations, but these equations are not taken into account the effect of the nanoparticle shape. Therefore, the new correlations are required to calculate the Nusselt number of nanofluids according to nanoparticle shape.

3.3. Nanoparticle shape effect on fluid flow characteristics

The nanoparticle shape effect on the pressure drop of nanofluids is shown in Figs. 10(a) and 10(b) in laminar and turbulent flow regimes, respectively.

It is seen that the pressure drop of nanofluids changes both with nanoparticle shape and with the Reynolds number as the platelet nanoparticle has the highest pressure drop compared with other nanoparticles.

As mentioned in the literature, the use of nanoparticles in the lubricants improves anti-abrasive properties and also reduces the destructive forces and friction factor [30]. Therefore, energy is saved, and the efficiency increases. According to Figs. 11(a) and 11(b), it is known that the friction factor depends on the nanoparticle shape. It is also

seen that the minimum and maximum friction factor is related to the platelet and spherical nanoparticles, respectively.

3.4. Proposed correlations

In traditional correlations such as Eqs. (17) and (18), the shape effect of nanoparticles has been not taken into account to calculate the heat transfer coefficient. This subject is led to a discrepancy between the simulation results and the suggested equations in the literature. Therefore, according to numerical simulations, two correlations are suggested to calculate the Nusselt number dependent on the shape of nanoparticles. It was assumed that the Nusselt number is a function of nanofluid thermophysical properties, flow characteristics, and nanoparticle shape as follows:

$$Nu = a\,\psi^b\left(\frac{Pr_{nf}}{Pr_{bf}}\right)^c Re^d \varphi^e \qquad (23)$$

The multivariate regression analysis in Polymath software version 6.10 was carried out to give the parameters a, b, c, d, and e. Finally, the following correlations were obtained to calculate the Nusselt number of CuO/water nanofluids:
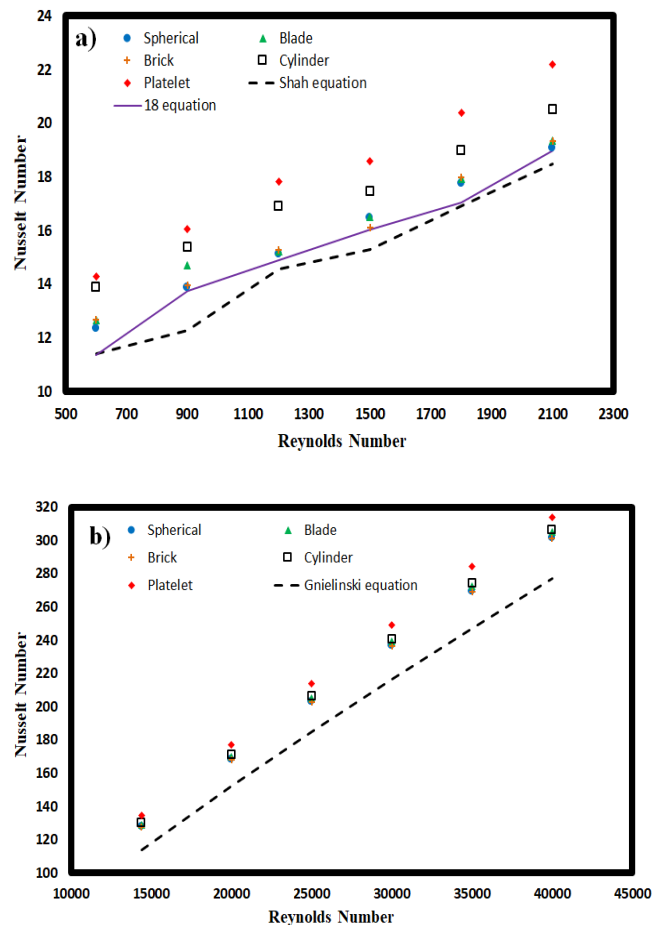

Figure 9. Effect of Reynolds number on Nusselt number with different nanoparticle shapes in 1 % nanoparticle volume fraction: a) Laminar flow b) Turbulent flow
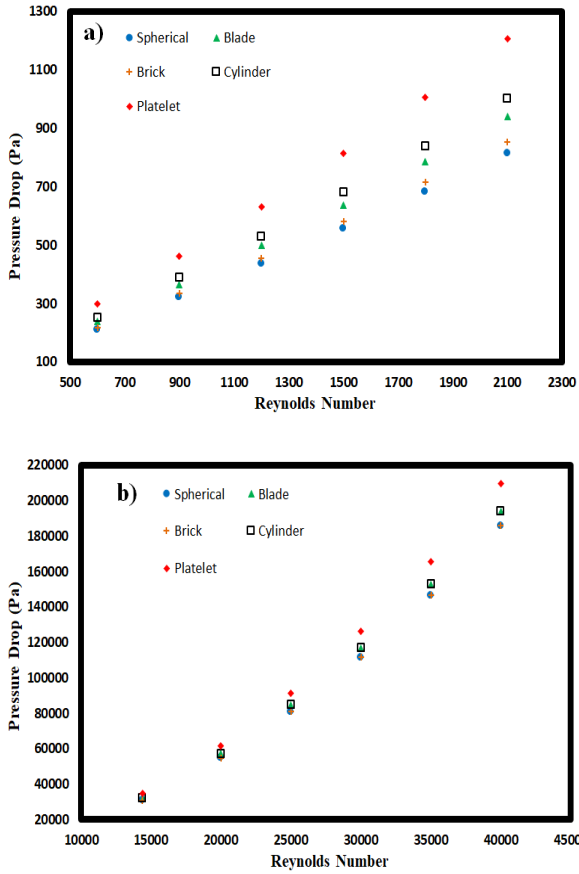
Figure 10. Effect of Reynolds number on pressure drop with different nanoparticle shapes in 1 % nanoparticle volume fraction: a) Laminar flow b) Turbulent flow

$$Nu = 1.03\psi^{0.018}(\frac{Pr_{nf}}{Pr_{bf}})^{0.04}Re^{0.39}\varphi^{0.3} \qquad \text{Laminar flow regime} \qquad (24)$$

$$Nu = 0.073\psi^{0.0088}(\frac{Pr_{nf}}{Pr_{bf}})^{0.825}Re^{0.82}\varphi^{0.28} \qquad \text{Turbulent flow regime} \qquad (25)$$

In these equations, ψ and φ are sphericity factor and volume fraction of nanoparticle, respectively.

The comparison of CFD simulations and Eqs. (24) and (25) have been carried out in Figs. 12 and 13, respectively. As can be seen in these figures, the Nusselt number of correlation has good agreement with that of the simulations. The maximum difference between the proposed correlations and CFD results is up to 10% and 5% in laminar and turbulent flow regimes, respectively.

4. Conclusions

The thermal performance and flow characteristics of CuO/water nanofluids in a mini tube with a circular cross-section under constant heat flux were numerically studied. The effect of nanoparticle shape was taken into account in CFD simulations. Five nanoparticles such as spherical, cylindrical, platelet, brick, and blade were studied. The

numerical results indicated that the heat transfer coefficient and Nusselt number of nanofluids would increase with the Reynolds number and volume fraction of nanoparticles. These characteristics for nanofluid containing platelet nanoparticles were the highest compared with other nanofluids. According to CFD simulations, it was found that the Nusselt number of nanofluid with platelet nanoparticle increases about 16% compared to that of the spherical nanoparticle. Furthermore, an increase up to 7.6%, 1.4% and 1% in nanofluids using cylindrical, blade and brick nanoparticles were observed, respectively.

The numerical results showed that the pressure drop of nanofluids increases with increasing the Reynolds number while their friction factor decreased with that. It was seen that the friction factor of the nanofluid containing the platelet nanoparticle is the least amount compared with other nanofluids. Finally, since the effect of nanoparticle shape has not been included in the conventional equations to calculate the Nusselt number of nanofluids, two correlations were proposed to calculate the heat transfer coefficient of nanofluids taken into account the effect of nanoparticle shape. The proposed correlations can predict the CFD simulations with a good degree of precision.
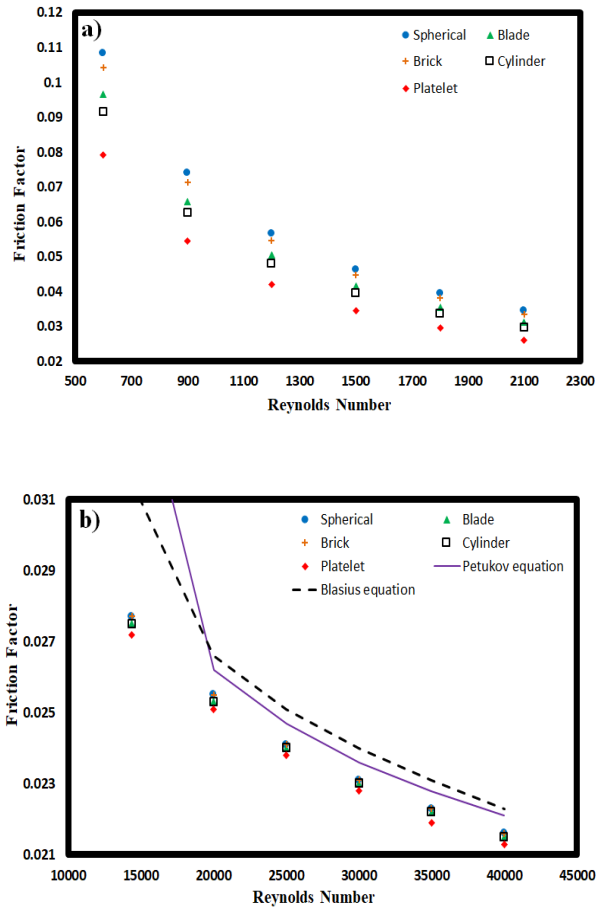

Figure 11. Effect of Reynolds number on friction factor with different nanoparticle shapes in 1 % nanoparticle volume fraction: a) Laminar flow b) Turbulent flow
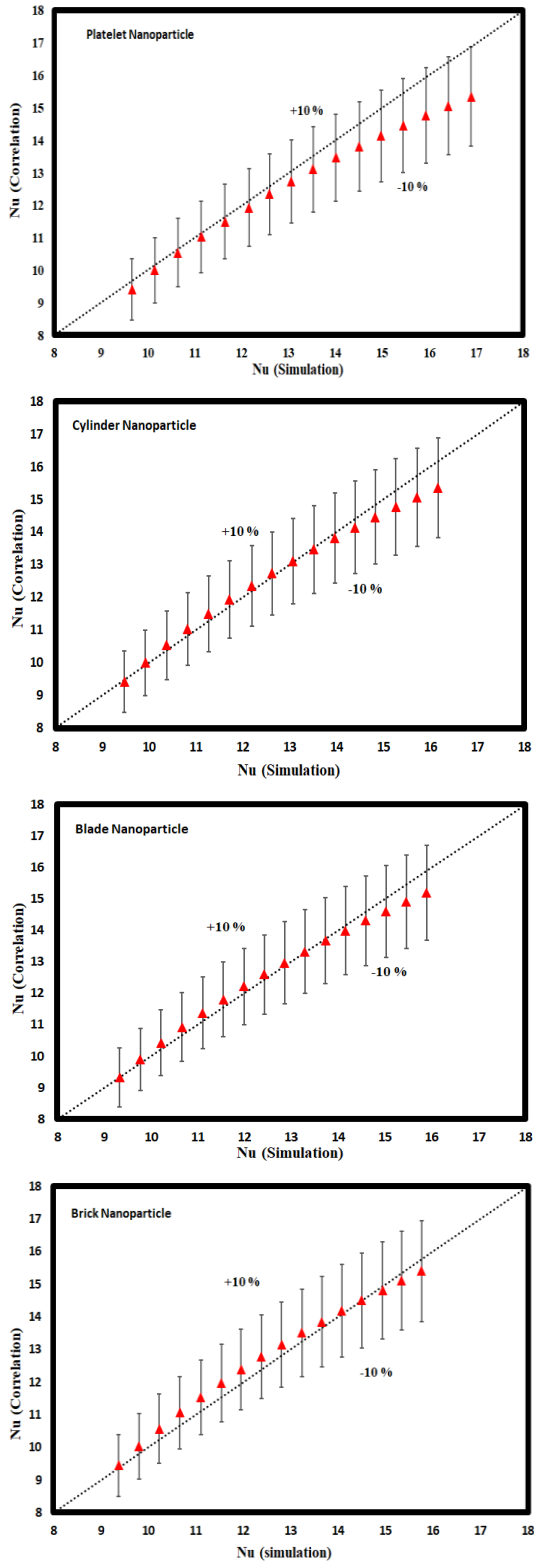
Figure 12. Comparison of Nusselt number of proposed correlation with CFD simulations in laminar flow regime with 0.4 % nanoparticle volume fraction
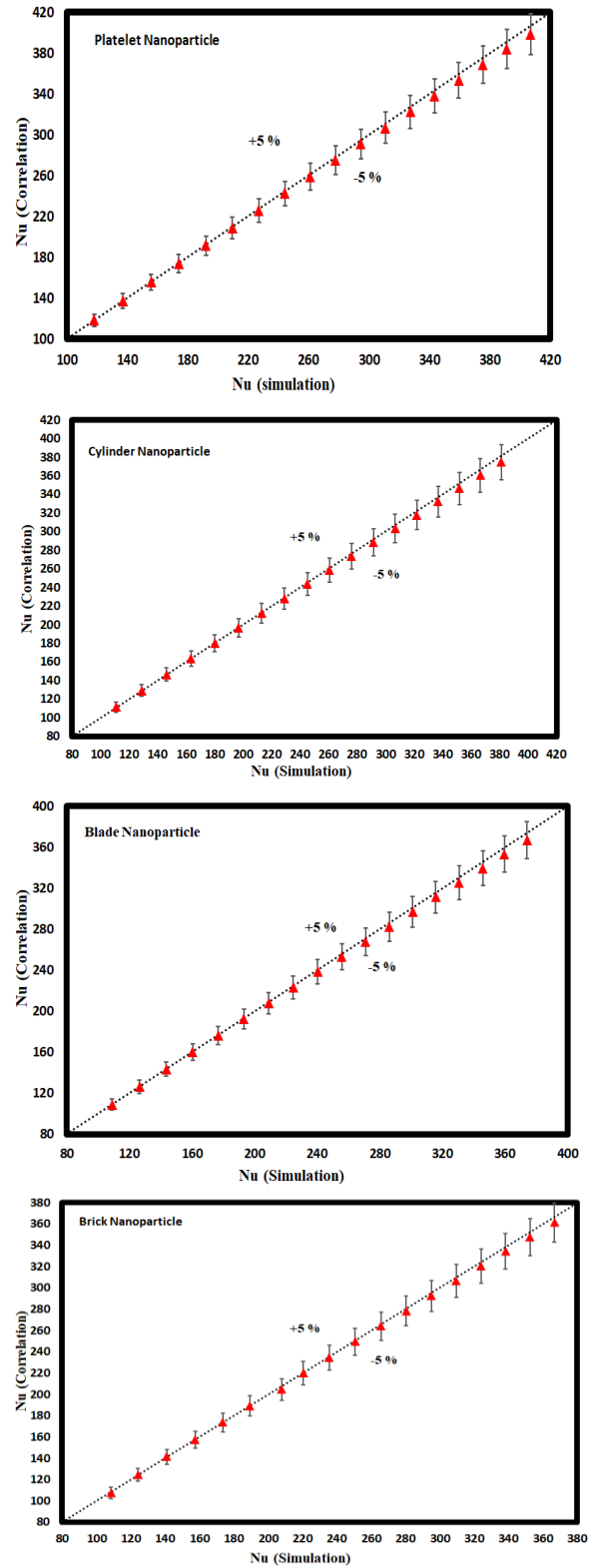

Figure 13. Comparison of Nusselt number of proposed correlation with CFD simulations in turbulent flow regime with 0.4 % nanoparticle volume fraction

Nomenclatures

C	Specific heat capacity, (J/ kg.°C)
d	Diameter, (m)
f	Friction factor
h	Heat transfer coefficient, (W/m^2.°C)
k	Thermal conductivity, (W/m.°C)
L	Length, (m)
n	Empirical shape factor
V	Velocity, (m/s)
x	Axial distance, (m)
Nu	Nusselt Number, Nu = (h D/k)
Pr	Prandtl Number, Pr = (Cμ/k)
Re	Reynolds Number, Re = (ρVD /μ)

Greek symbols

ρ	Density, (kg/m^3)
μ	Viscosity, (N.s/m^2)
ψ	Sphericity factor
φ	Volume fraction
ΔP	Pressure drop, (N/m^2)

Subscripts

f	Fluid
p	Particle
bf	Base fluid
nf	Nanofluid
w	Wall

References

[1] G. Roy, C.T. Nguyen, P.R. Lajoie, Numerical investigation of laminar flow and heat transfer in a radial flow cooling system with the use of nanofluids, Superlattices and Microstructures, 35, 497-511, (2004).

[2] S. Sundar, L. Singh, K. Manoj, Convective heat transfer and friction factor correlations of nanofluid in a tube and with inserts-A review, Renewable and Sustainable Energy Reviews, 20, 23-35, (2013).

[3] G. Pathipakka, P. Sivashanmugam, Heat transfer behaviour of nanofluids in a uniformly heated circular tube fitted with helical inserts in laminar flow, Superlattices and Microstructures, 47, 349-360, (2010).

[4] S.E.B. Maïga, C.T. Nguyen, N. Galanis, G. Roy, Heat transfer behaviours of nanofluids in a uniformly heated tube, Superlattices and Microstructures, 35, 543-557, (2004).

[5] K.H. Solangi, S.N. Kazi, M.R. Luhur, A. Amiri, R. Sadi, M.N.M. Zubir, S. Gharehkhani, K.H. Teng, A comprehensive review of thermo-physical properties and convective heat transfer to nanofluids, Energy, 89, 1065-1086, (2015).

[6] S.M. Vanaki, P. Ganesan, H.A. Mohammed, Numerical study of convective heat transfer of nanofluids-A review, Renewable and Sustainable Energy Reviews, 54, 1212-1239, (2016).

[7] W. Zhong, A. Yu, X. Liu, Z. Tong, H. Zhang, DEM/CFD-DEM modelling of non-spherical particulate systems: theoretical developments and applications, Powder Technology, 302, 108-152, (2016).

[8] H. Xie, J. Wang, T. Xi, Y. Liu, Thermal conductivity of suspensions containing nanosized SiC particles, International Journal of Thermophysics, 23, 571–580, (2002).

[9] S.M.S. Murshed, K.C. Leong, C. Yang, Enhanced thermal conductivity of TiO2-water based nanofluids, International Journal of Thermal Sciences, 44, 367-373, (2005).

[10] E.V. Timofeeva, J.L. Routbort, D. Singh, Particle shape effects on thermophysical properties of alumina nanofluids, Journal Of Applied Physics, 106, 014304, (2009).

[11] M.M. Elias, M. Miqdad, I.M. Mahbubul, R. Saidur, M. Kamalisarvestani, M.R. Sohel, A. Hepbasli, N.A. Rahim, M.A. Amalina, Effect of nanoparticle shape on the heat transfer and thermodynamic performance of a shell and tube heat exchanger, International Communications in Heat and Mass Transfer, 44, 93-99, (2013).

[12] S.M. Vanaki, H.A. Mohammed, A. Abdollahi, M.A. Wahid, Effect of nanoparticle shapes on the heat transfer enhancement in a wavy channel with different phase shifts, Journal of Molecular Liquids, 196, 32-42 (2014).

[13] J.Z. Lin, Y. Xia, X. K. Ku, Flow and heat transfer characteristics of nanofluids containing rod-like particles in a turbulent pipe flow, International Journal of Heat and Mass Transfer, 93, 57-66, (2016).

[14] M. Bahiraei, R. Khosravi, S. Heshmatian, Assessment and optimization of hydrothermal characteristics for a non-Newtonian nanofluid flow within miniaturized concentric-tube heat exchanger considering designer's viewpoint, Applied Thermal Engineering, 123, 266–276, (2017).

[15] P. Naphon, S. Wiriyasart, Experimental study on laminar pulsating flow and heat transfer of nanofluids in micro-fins tube with magnetic fields, International Journal of Heat and Mass Transfer, 118, 297–303, (2018).

[16] M. Bahiraei, N. Mazaheri, Application of a novel hybrid nanofluid containing graphene–platinum nanoparticles in a chaotic twisted geometry for utilization in miniature devices: Thermal and energy efficiency considerations, International Journal of Mechanical Sciences, 138–139, 337–349, (2018).

[17] D. Wen, Y. Ding, Experimental investigation into convective heat transfer of

nanofluids at the entrance region under laminar flow conditions, International Journal of Heat and Mass Transfer, 47, 5181-5188, (2004).

[18]   M. Hatami, M. Jafaryar, J. Zhou, D. Jing, Investigation of engines radiator heat recovery using different shapes of nanoparticles in H2O/(CH2OH)2 based nanofluids, International Journal of Hydrogen Energy, 42, 10891-10900, (2017).

[19]   R. Deepak Selvakumar, S. Dhinakaran, Forced convective heat transfer of nanofluids around a circular bluff body with the effects of slip velocity using a multi-phase mixture model, International Journal of Heat and Mass Transfer, 106, 816-828, (2017).

[20]   A. Behzadmehr, M. Saffar-Avval, N. Galanis, Prediction of turbulent forced convection of a nanofluid in a tube with uniform heat flux using a two-phase approach, International Journal of Heat and Fluid Flow, 28, 211-219, (2007).

[21]   A.R. Moghadassi, E. Ghomi, F. Parvizian, A numerical study of water based Al2O3 and Al2O3-Cu hybrid nanofluid effect on forced convective heat transfer, International Journal of Thermal Sciences, 92, 50-57, (2015).

[22]   M. Manninen, V.Taivassalo, S. Kallio, On the mixture model for multiphase flow, VTT Publications, Technical Research Center of Finland, 288, (1996).

[23]   L. Schiller, A. Naumann, A drag coefficient correlation, Z. Ver. Deutsch. Ing, 77, 318-320, (1935).

[24]   A. Hussanan, M.Z. Salleh, I. Khan, S. Shafie, Convection heat transfer in micropolar nanofluids with oxide nanoparticles in water, kerosene and engine oil, Journal of Molecular Liquids, 229, 482-488, (2017).

[25]   Y. Xuan, W. Roetzel, Conceptions for heat transfer correlation of nanofluids, International Journal of Heat and Mass Transfer, 43, 3701-3707, (2000).

[26]   R.K.Shah, Thermal entry length solutions for the circular tube and parallel plates, Proceedings of 3rd National Heat and Mass Transfer Conference, Indian Institute of Technology, Bombay, 1175, (1975).

[27]   V. Gnielinski, New equations for heat and mass transfer in turbulent pipe and channel flow, International Chemical Engineering, 16, 359-368, (1976).

[28]   F.M. White, Fluid Mechanics, eighth ed., McGraw-Hill Eduction, New York, (2016).

[29]   B.S. Petukhov, Heat transfer and friction in turbulent pipe flow with variable physical properties, Advances in Heat Transfer, 6, 503-564, (1970).

[30]   D. K. Devendiran, V.A. Amirtham, A review on preparation, characterization, properties and applications of nanofluids, Renewable and Sustainable Energy Reviews, 60, 21-40, (2016).